Studies on Profile Loss Associated with Wake-Disturbed Unsteady Boundary Layer on a Flat Plate

Ken-ichi Funazaki
Department of Mechanical Engineering
Iwate University
Morioka, Japan

Tadashi Tanuma
Heavy Apparatus Engneering Laboratory
Toshiba Corporation
Yokohama, Japan

SYNOPSIS

The present study contains experimental works on a flat-plate boundary layer disturbed by periodic incoming wakes. Special interest is focused on effects of the wake passing upon the profile loss associated with the boundary layer. A spoked-wheel type wake generator is employed to simulate the incoming wakes. Time-resolved behaviors of the wake-affected boundary layer are measured by a hot-wire probe, which yields the time-resolved and time-averaged integral parameters of the boundary layer. These experimental data are compared with the estimations calculated with the method that is originally based on Hodson's method [(1)], being modified to account for arbitrary propagation speed of the turbulent patches.

NOTATION

C_D, C_f	:	dissipation coefficient, skin-friction coefficient
d	:	diameter of the wake generating bar
f	:	wake passing frequency($= nn_b/60$)
L	:	characteristic length (= plate length)
l_D	:	streamwise gap between a wake-generating bar and the plate leading edge
n, n_b	:	rotational speed, number of wake-generating bars
Re_x, Re_θ	:	local Reynolds number ($=U_\infty x/\nu$), momentum thickness Reynolds number
S	:	Strouhal number ($= fL/U_\infty$)
$s, \Delta s$	:	entropy, total entropy generation
T	:	temperature
$Tu_{\max}$	:	maximum turbulence intensity in the wake
t	:	time
U_∞, U_e	:	inlet velocity, velocity at the edge of the boundary layer
U_m	:	bar moving speed
$u(t), \tilde{u}(t)$	:	instantaneous and ensemble-averaged velocities
x	:	distance measured from the plate leading edge
x_{tw}	:	location where a wake-induced transition initiates
$\delta_1, \delta_2, \delta_3$	:	displacement, momentum, energy dissipation thickness
τ	:	wake passing period($=1/f$)
$\tau_{1/2}, \tau_w$	:	semi-depth width of the wake profile, wake duration
ν	:	kinematic viscosity
ζ	:	loss coefficient

subscript

e	:	edge of the boundary layer
L, T	:	end of laminar flow, start of turbulent flow
t, tw	:	end of transition, forced transition point by wake

superscript

$\bar{f}, f$	:	time-averaged, ensemble-averaged

INTRODUCTION

It is well understood that wakes from the upstream blade cascade significantly affect the boundary layer on the following blade surface, resulting in early boundary-layer transition or causing a noticeable change in blade profile loss. One of the earliest studies concerning the wake-affected blade profile loss was made by Lopatitskii[2] using an axial turbine stage, followed by Pfeil and Herbst[3] or Hodson[4]. They found that the wake passage seriously deteriorated the cascade aerodynamic performance in comparison with the steady-state performance. Despite recent progresses in CFD techniques, it is still difficult to make an accurate prediction of the cascade performance even under the steady-state flow condition. Accordingly a reliable correlation is inevitable for aerodynamists of turbomachines to evaluate the effect of the wake passing on the cascade performance. Scholz[5] published the experimental data concerning the unsteady cascade loss, which were originally produced by Speidel[6] using a single airfoil under the influence of incoming wakes generated by an oscillating wire. Sharma et al.[7] rearranged these data, including the above-mentioned data of Pfeil and Herbst [3] as well as Hodson[4], against his unsteadiness parameter. It was demonstrated in their study that a correlation for the loss estimation could be deduced from those data, regardless of whether or not such a correlation had any physical meanings, though. Taking advantage of the distance-time diagram of the wake-affected boundary layer, Hodson[1] then developed a rational model that successfully explained the tendency of the previous experimental data.

In the present study detailed measurements of wake-affected boundary layers on a flat plate are conducted using a hot-wire probe. The experimental setup is almost the same as the previous study by Funazaki[8], in which a spoked-wheel type wake generator is used to simulate incoming periodic wakes. The obtained data are then processed to have the integral parameters for the boundary layer, e.g., the energy dissipation thickness, which is compared with the estimations by a method that is originated from Hodson's model, incorporated with a newly developed model to account for arbitrary propagation speed of the turbulent patches.

EXPERIMENTAL SETUP

Test Apparatus

Figure 1 presents the test apparatus, of which configuration is the same as that of the previous study done by Funazaki[8]. Air from the blower, passing through the settling chamber and the contraction nozzle, enters the transition duct with turbulence level less than 0.5%. The test channel with sharp-edged front ends is inserted into the duct, having a clearance between the channel and the duct for the purpose of discharging some amount of air so as to obtain uniform inflow into the test duct. The test plate of 1000 mm length and 10 mm thickness is horizontally installed inside the test channel along the channel center line. Since the test plate has sharp-edged leading edges, the inflow becomes slightly asymmetric about the plate center line and there might be a possibility of flow separation arising at the leading edge. A flow controlling device is therefore equipped at the rear end of the test plate to avoid this problem. Smooth inlet flow condition to the test plate is consequently obtained, being confirmed by an oil-flow pattern as well as a tuft motion.

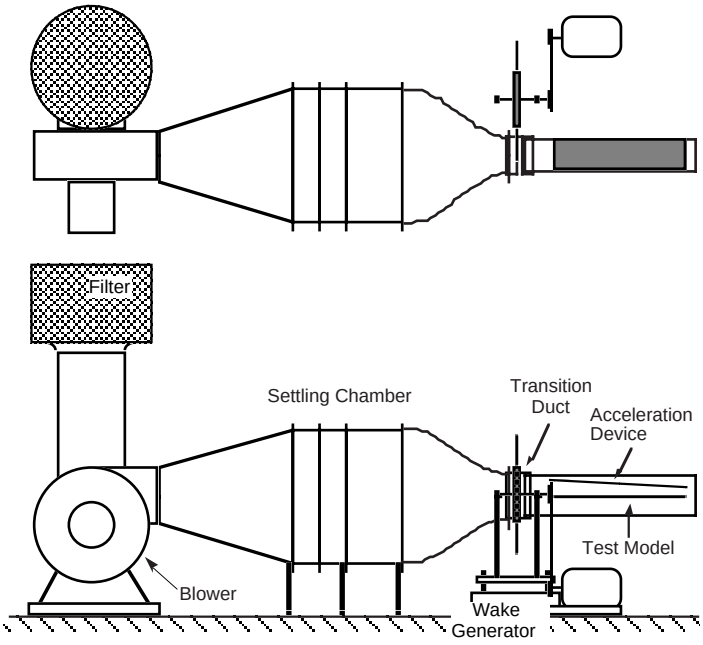

Figure 1 Test apparatus

A spoked-wheel type wake generator is used to make the wake-disturbed inlet flow to the test plate. Cylindrical bars of 250 mm length and 5 mm diameter are attached to the disk rim of the wake

generator. The bars generate wakes behind them while passing across the inlet flow. The streamwise distance between the locus of the bars and the plate leading edge (l_D) is 200 mm. A rotation speed n is controlled with the transmission gear box, being monitored with an optical tachometer. Rotation direction of the wake generator can be changed so that it generates two types of the wakes that affect the boundary layer on the test surface in different manners, as shown in Figure 2. When one of the bars moves downward in front of the plate ('normal rotation' case), it generates the wake that impinges the test surface. On the other hand, when the bar goes upward ('reverse rotation' case), it produces the wake that leaves the test surface.

Due to the structure of the wake generator, the bar-generated wakes contain three-dimensional structure along the radial direction. A great care is therefore paid to the location of the wake generator relative to the test plate. The disk axis is situated at almost the same height with the plate surface from the ground, so that each of the bars becomes aligned with the test plate leading edge when it moves just ahead of the plate. This arrangement makes it possible to achieve nearly two-dimensional impact of the wakes upon the boundary layer over the test plate because most of the wakes that will affect the boundary layer are generated just upstream of the plate and convected downstream by the uniform flow within the duct.

Instruments and Data Processing

Figure 2 shows the system for the boundary layer measurement. An I-type hot-wire probe (Kanomax, Model 0251R) is traversed at several streamwise locations to obtain instantaneous velocity data inside the boundary layer. The data processing system consists of a CTA with a linearizer (Kanomax, System 7201), an A/D convertor (Autonix, APC-204) and a PC for controlling the system. Data sampling frequency is 50 kHz. Each of the data-acquisition processes is triggered with a pulse from the optical tachometer, which makes test data synchronized with the disk revolution. These digitized velocity data for each traversing location, $u_i(y,t_j)$ $(j=1,...,2048)$, are then used to calculate an ensemble-averaged velocity $\tilde{u}_i(y,t_j)$ and a local turbulence intensity $Tu(t_j)$ as follows;

$$\tilde{u}(y,t_j)=\frac{1}{k}\sum_{i=1}^{k}u_i(y,t_j)\ , \qquad Tu(t_j)=\sqrt{\frac{1}{k-1}\sum_{i=1}^{k}\left[u_i(t_j)-\tilde{u}(t_j)\right]^2}\Big/U_\infty\ ,\quad k=256\,. \tag{1}$$

Integral Parameters

From the ensemble-averaged velocity data, the integral parameters for the wake-affected boundary layer are calculated by the following equations,

displacement thickness $$:\tilde{\delta}_1(t)=\int_0^{\tilde{\delta}(t)}\left(1-\left\{\frac{\tilde{u}(y,t)}{\tilde{U}_e(t)}\right\}\right)dy\ , \tag{2}$$

momentum thickness $$:\tilde{\delta}_2(t)=\int_0^{\tilde{\delta}(t)}\left\{\frac{\tilde{u}(y,t)}{\tilde{U}_e(t)}\right\}\left(1-\left\{\frac{\tilde{u}(y,t)}{\tilde{U}_e(t)}\right\}\right)dy\ , \tag{3}$$

energy dissipation thickness $$:\tilde{\delta}_2(t)=\int_0^{\tilde{\delta}(t)}\left\{\frac{\tilde{u}(y,t)}{\tilde{U}_e(t)}\right\}\left(1-\left\{\frac{\tilde{u}(y,t)}{\tilde{U}_e(t)}\right\}^2\right)dy\ , \tag{4}$$

where $\tilde{\delta}(t)$ is the ensemble-averaged boundary layer thickness, at which the velocity $\tilde{u}(y,t)$ reaches a maximum, say, $\tilde{U}_e(t)$. In addition, the shape factors are determined by

$$\tilde{H}_{12}(t)=\frac{\tilde{\delta}_1(t)}{\tilde{\delta}_2(t)}\ ,\quad \tilde{H}_{32}(t)=\frac{\tilde{\delta}_3(t)}{\tilde{\delta}_2(t)} \tag{5}$$

Uncertainty

Uncertainty analyses are made according to the standard procedure by Kline and McClintock[9], which reveals that the average uncertainty in the energy dissipation thickness was about $\pm 12\%$.

BOUNDARY LAYER LOSS

Theoretical Background

Denton[10] developed a systematic approach to define loss coefficient ζ by introducing the concept of entropy generation, which yields

$$\zeta = \frac{T_2 \Delta s}{m\left(h_{02} - h_0\right)} = \frac{T_2 \Delta s}{m U_2^2 / 2} , \qquad (6)$$

where Δs is a total entropy generation through a process, and m is a mass-flow rate. Introducing an entropy thickness δ_s, Denton presented an expression for entropy generation in a two-dimensional boundary layer as follows;

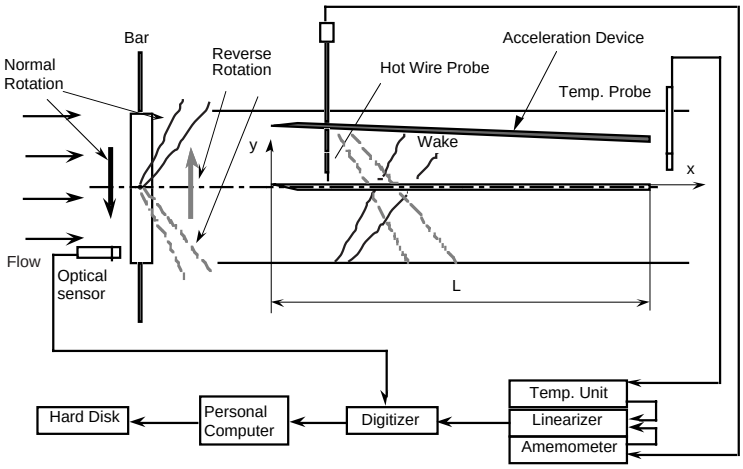

Figure 2 Test section and measurement system

$$\Delta s = \frac{\rho_e U_e^3 \delta_s}{T_e} \text{ , where } \delta_s = \frac{T_e}{\rho_e U_e^3} \int_0^{\delta} \rho u \left(s - s_e\right) dy \ . \qquad (7)$$

Considering that the flow is almost incompressible for the present case and the entropy thickness accordingly becomes identical to the energy dissipation thickness in the low speed flow, one can obtain the following expression for the boundary layer loss observed at $x = x_{ref}$,

$$\zeta = \zeta\left(x_{ref}\right) = 2\rho_\infty U_\infty \delta_3\left(x_{ref}\right) / m \ . \qquad (8)$$

Generalized Hodson's method

Using distance-time diagrams for wake affected boundary layer states, as shown in Figure 3, Hodson[1] proposed several models for estimation of the boundary layer loss. Hodson assumed $\beta_F \cong 1.0$ and $\beta_E \cong 0.5$, where β_F and β_E are propagation speed ratios of the leading and trailing edges of the wake-induced turbulent patch, which is depicted by a hatched region in Fig. 3. His expression can be generalized for arbitrary values for β_F and β_E as follows;

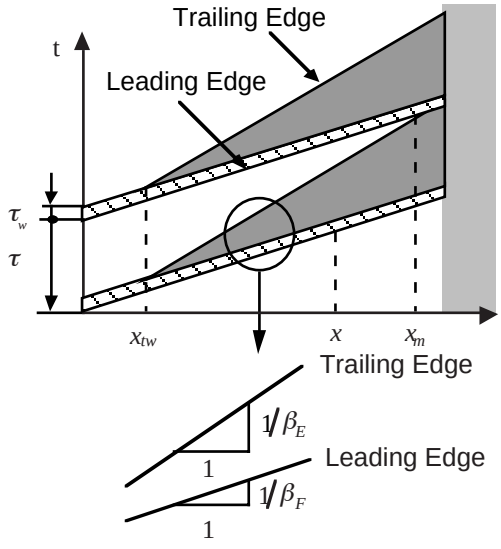

Figure 3 Distance-time diagram of the wake-affected boundary layer

$$\frac{\bar{\xi} - \xi_L}{\xi_T - \xi_L} = 1 - \frac{1}{2}\frac{2\pi\phi}{\bar{\omega}}\left(1 - \frac{\tau_w}{\tau}\right)^2 \ , \quad \frac{\bar{\omega}}{2\pi\phi} \geq 1 - \frac{\tau_w}{\tau}$$
$$= \frac{1}{2}\frac{\bar{\omega}}{2\pi\phi} + \frac{\tau_w}{\tau} \ , \quad \frac{\bar{\omega}}{2\pi\phi} \leq 1 - \frac{\tau_w}{\tau} \qquad (9)$$
$$\phi = \frac{\beta_E}{\beta_F - \beta_E} \ , \quad \bar{\omega} = \frac{2\pi f\left(x_t - x_{tw}\right)}{U_\infty} = \frac{2\pi\left(x_t - x_{tw}\right)}{L} S$$

where $\bar{\xi}$ is a loss coefficients for the wake-affected boundary layer and $\bar{\omega}$ is a reduced frequency, using the distance between the transition onset (x_{tw}) and the end of the transition (x_t) as characteristic length. $\bar{\xi}_L$ and $\bar{\xi}_T$ are loss coefficients associated with steady boundary layers in which the transition initiates at x_{tw} and x_t, respectively. Lumping the right-hand-side of Eq. (12) as $F\left(\bar{\omega}, \tau_w/\tau\right)$ and substituting Eq. (8) into Eq. (9), we have the expression for the wake-affected energy dissipation thickness as follows;

$$\bar{\delta}_3 = \delta_{3,L} + F\left(\bar{\omega}, \tau_w/\tau\right)\left(\delta_{3,T} - \delta_{3,L}\right) , \qquad (10)$$

where $\delta_{3,L}$ and $\delta_{3,T}$ are determined with Eq. (A.11) as shown in Appendix, incorporating a virtual origin of the turbulent boundary layer into the formulation. From Eqs. (8) and (10) one can predict the additional loss caused by the wake passing over the boundary layer, the losses associated with laminar and turbulent boundary layers being specified. In such a case, wake duration τ_w and wake-induced transition onset x_w are also to be specified. A relevant discussion on this point was made by Funazaki[11]. He regarded the period over which more than 4% turbulence intensity lasted in the incoming wake as wake duration τ_w. Approximating the wake turbulence profile as a Gaussian distribution, τ_w is given by

$$\tau_w = 3.36\tau_{1/2}\sqrt{-\ln\left(4/Tu_{\max}\right)}\ , \tag{11}$$

$$\tau_{1/2} \cong 1.5 \times \frac{0.308\sqrt{C_d d\, l_D/\cos\lambda_w}}{U_m \cos\lambda_w}\ ,\quad \lambda_w = \tan^{-1}\left(U_m/U_\infty\right) \tag{12}$$

As for the transition onset, a quasi-steady approach using the criterion of Abu-Ghannam and Shaw[12] is adopted in this study for simplicity, which is

$$Re_{\theta,w} = 163 + \exp\left(6.91 - Tu_{\max}\right)\ ,\ Re_{\theta,tw} = U_\infty \delta_{2,tw}/\nu\ . \tag{13}$$

Comparison with the previous data

Figure 4 shows the experimental data by Speidel[6] and Pfeil and Herbst[3]. Also shown are the estimations by use of Eq. (9) with $\beta_E = 0.5$ (adopted by Hodson[1]) and $\beta_E = 0.55$, as suggested by Funazaki[8]. Note that the data of Speidel designated as 'kanal II' are not used in this case because those data were obtained under a relatively large flow acceleration that is not taken into account in Eq. (9). Both estimations almost follow the experimental data, however, the estimation with $\beta_E = 0.55$ seems to provide better result in comparison with the curve of $\beta_E = 0.5$.

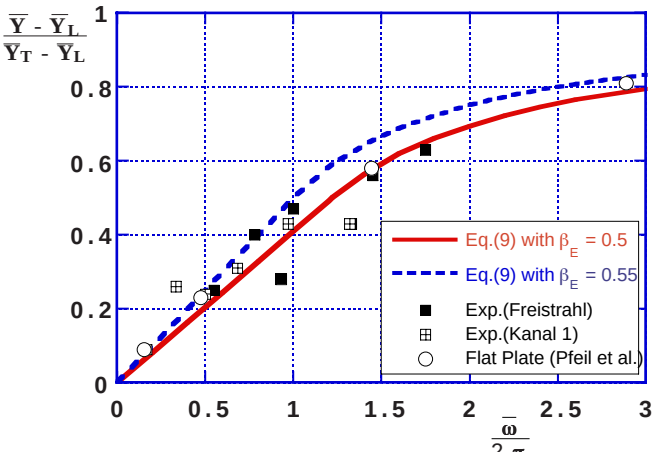

Figure 4 Comparison of the generalized Hodson's model and experimental data

RESULTS

Time-Resolved Behaviors of the Boundary Layer

Figure 5 shows some examples of the time-resolved characteristics of the wake-affected boundary layer for $S = 2.83$. At $x/L = 0.10$, the boundary layer thicknesses rapidly increase and the shape factor $\tilde{H}_{12}$ accordingly decreases almost to the full turbulent level ($\cong 1.4$) as the wake passes over the boundary layer. At $x/L = 0.60$, where the transition process seems to be almost completed from the viewpoint of the time-averaged shape factor, the boundary layer thicknesses still vary with the wake passage. Figure 6 demonstrates the time-resolved characteristics of the wake-affected boundary layer for the highest wake passing frequency ($S = 5.65$). In this case the merger between the two neighboring turbulent regions is expected to occur around at $x/L = 0.20$. This suggests that the boundary layer reaches a full turbulent condition by $x/L = 0.60$, which can be confirmed by the behavior of $\tilde{H}_{12}$ in Figure 6. However, as shown also in Figure 6, the three boundary layer thicknesses exhibit sinusoidal behaviors due to the wake passing over the boundary layer. Similar findings are already reported by Schobeiri et al.[13]

Time-Averaged Behaviors of the Boundary Layer

Time-averaged quantities are defined as

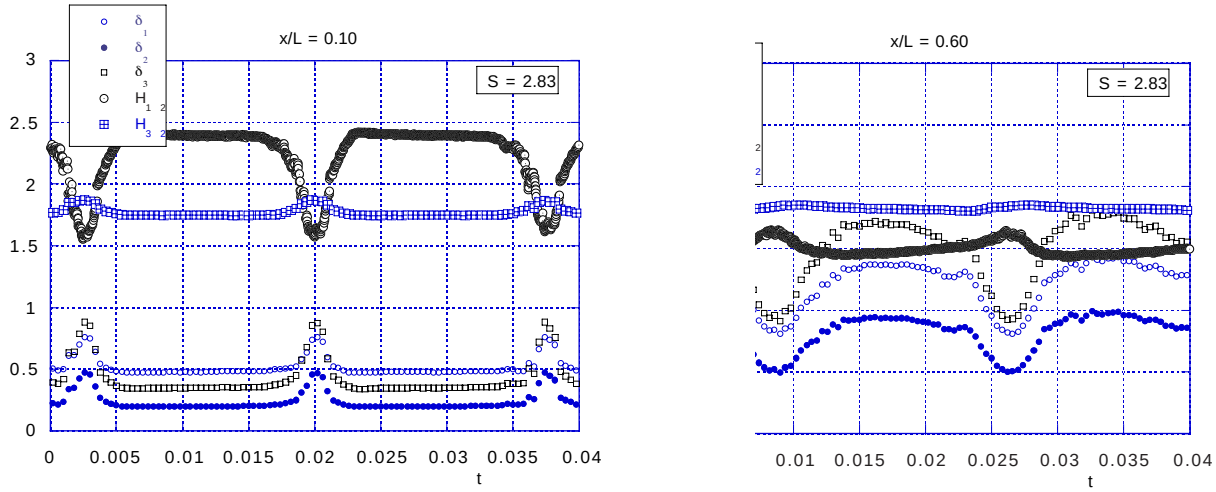

Figure 5 Time-resolved characteristics of the wake-affected boundary layer (S = 2.83) (left) x/L = 0.10 (right) x/L = 0.60

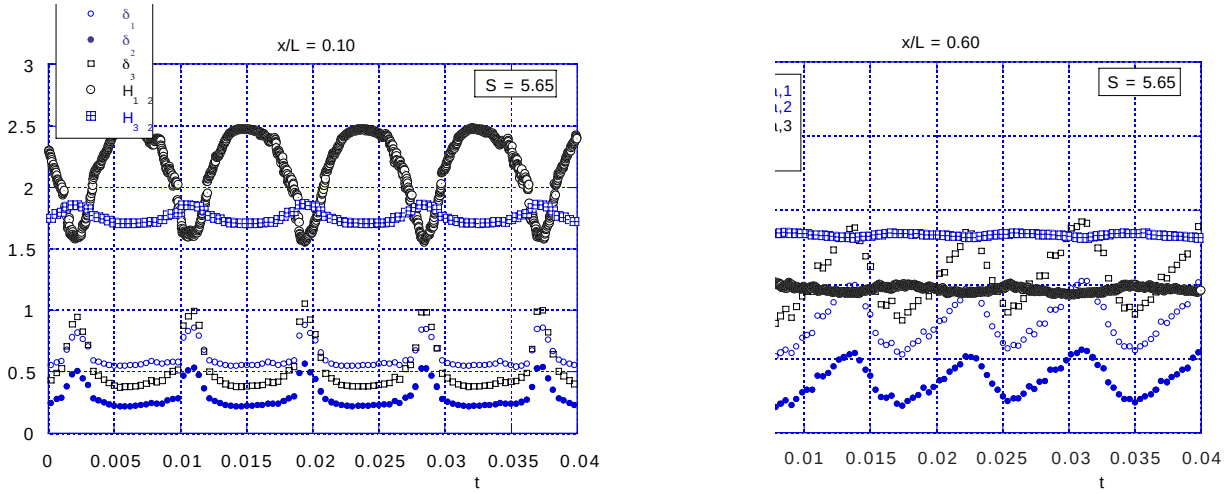

Figure 6 Time-resolved characteristics of the wake-affected boundary layer (S = 5.65) (left) x/L = 0.10 (right) x/L = 0.60

$$\bar{f} = \frac{1}{\tau}\int_0^{\tau} \tilde{f}(t)dt \ . \qquad (14)$$

Figure 7 shows streamwise variations of the time-averaged energy dissipation thickness $\bar{\delta}_3$ obtained for several unsteady flow conditions, where open and solid symbols represent the data for 'normal rotation' and 'reverse rotation' cases, respectively. The energy dissipation thickness becomes larger as the Strouhal number increases, which demonstrates a salient effect of the wake passing upon the boundary layer loss as indicated by the loss model (Eq. (9)). It is also evident that there appear differences between the data of 'normal rotation' and 'reverse rotation' cases. From the observation of the time-resolved behavior of the wake-affected boundary layer, it is found that the wake duration for the 'reverse rotation' case is meaningfully shorter than that of the 'normal rotation' case. Furthermore, the wake near the plate surface for the reverse rotation' case tends to diminish as it is convected along with the flow. Therefore those differences in energy dissipation thickness can be attributed to the relative movement of the fluid within the wake, in other words, a negative jet effect as proposed by Kerrebrock and Mikolajczak[14]. However, further studies are needed to clarify the detail of the negative jet effect on the boundary layer transition.

These experimental data can be compared with the estimation given by Eq. (10) so as to check the validity of the loss model (Eq. (9)). Selecting $x/L = 0.60$ as the reference position (x_{ref}) for $\bar{\delta}_3$, we obtain the solid line as depicted in Figure 8 with experimental data, where $x_{tw} \cong 0.05$ and $x_t \cong 0.50$. One can see a large difference between the estimation given by Eq. (10) and the experiment, while the dependencies of the time-averaged thickness on the reduced frequency $\bar{\omega}$ resembles each other . Small modifications of the loss model, in particular, neglecting the wake duration, seemingly succeed in reduction of the discrepancy between the estimation and the experiment, regardless of whether or not they are physically acceptable modifications. Besides, one should bear in mind that the loss model, originally developed by Hodson[1], assumes that a quasi-steady approach holds even for high reduced frequency of the wake passing, which might be highly questionable and could be one of the reasons for relatively large disagreement observed at the highest reduced frequency among the present test conditions. As already seen in Figure 6, the energy dissipation thickness varies due to the wake passing over the boundary layer at the location where the shape factor indicates the boundary layer is of full turbulent state. The authors believe that such a dynamic behavior of the wake-affected boundary layer should be taken into account in the loss model in order to improve its predictive capability.

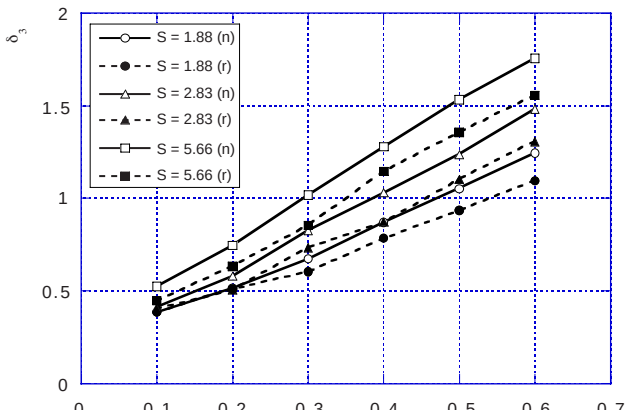

Figure 7 Time-averaged energy dissipation thickness for several unsteady conditions

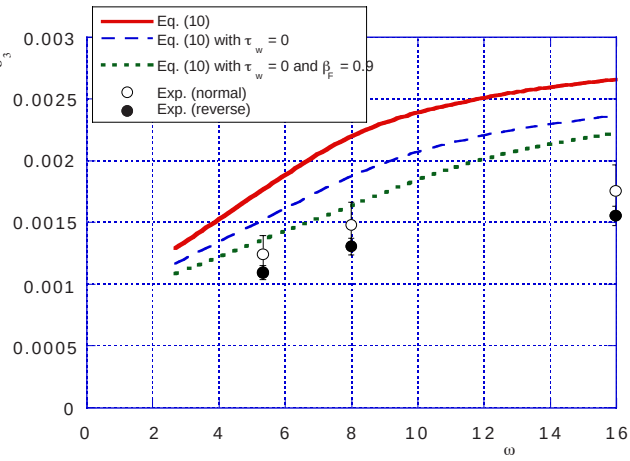

Figure 8 Wake-affected energy dissipation thickness at x/L = 0.6 and the estimation

CONCLUSIONS

Experimental works were executed to investigate the loss generation associated with a flat-plate boundary layer disturbed by periodic incoming wakes. A model for the wake-induced enhancement of the boundary layer loss, which was originally proposed by Hodson, was modified to account for arbitrary propagation speed of the turbulent patches, and the loss estimations were compared with the present experimental data. Summary of this paper is as follows:

(1) The integral parameters of the wake-affected boundary layer (displacement thickness, momentum thickness and energy dissipation thickness) exhibited sinusoidal behaviors due to the wake passing even at the location where the shape factor indicated the boundary layer reached a full turbulent condition.
(2) Time-averaged energy dissipation thickness increased with the Strouhal number.
(3) There arose a meaningful difference in time-averaged energy dissipation thickness between the normal and reverse rotation cases.
(4) The loss model developed in this study overestimated the energy dissipation thickness in comparison with the experiment, especially for the highest reduced frequency case. Although a slight improvement on the predictive capability of the model is seemingly possible by ways of tuning the parameters (wake duration, for example), it is worth while pursuing a more systematic approach for the improvement.

ACKNOWLEDGMENT

The authors are greatly indebted to Dr. T. Meguro, Mr. Y. Yamashita, Mr. T. Kitazawa, Mr. Y. Sasaki and Mr. K. Koizumi for their invaluable contributions to the present study.

REFERENCES

(1) Hodson, H. P., Modeling Unsteady Transition and Its Effect on Profile Loss, Trans. ASME Journal of Turbomachinery, 1990, Vol. 112, pp. 619-701.
(2) Lopatitskii, A. O., Energy Losses in the Transient State of an Incident Flow on the Moving Blades of Turbine Stages, Teploenergetika, 1970, Vol. 17, pp. 21-23.
(3) Pfeil, H. and Herbst, R., Transition Procedure of Instationary Boundary Layer, ASME Paper 79-GT-128, 1979
(4) Hodson, H. P., Measurements of Wake Generated Unsteadiness in the Rotor Passages of Axial Flow Turbines, ASME Paper 84-GT-189, 1984
(5) Scholz, N., Aerodynamics of Cascades, AGARD-AG-220, 1977, AGARD
(6) Speidel, L., Beeinflussuns der Laminarem Crezschicht durch Periodische Stronungen der Zustromung, Flugwiss, 1957, Vol. 9,
(7) Sharma, O. P., Renaud, E., Butler, T. L., Milsaps, J., K., Dring, R. P. and Joslyn, H. D., Rotor-Stator Interaction in Multi-Stage Axial-Flow Turbines, 24th AIAA/ASME/SAE/ASEE Joint Propulsion Conference, Boston, Massachusetts, 1988
(8) Funazaki, K., Unsteady Boundary Layers on a Flat Plate Disturbed by Periodic Wakes: Part II - Measurement of Unsteady Boundary Layers and Discussion, Trans. ASME Journal of Turbomachinery, 1996, Vol. 118, pp. 337-346.
(9) Kline, S. J. and McClintock, F. A., Describing Uncertainties in Single Sample Experiments, Mechanical Engineering, 1953, Vol. 75, pp. 3 - 8.
(10) Denton, J. D., Loss Mechanisms in Turbomachines, Trans. ASME Journal of Turbomachinery, 1993, Vol. 115, pp. 621 - 656.
(11) Funazaki, K., Unsteady Boundary Layers on a Flat Plate Disturbed by Periodic Wakes: Part I - Measurement of Wake-Affected Heat Transfer and Wake-Induced Transition Model, Trans. ASME Journal of Turbomachinery, 1996, Vol. 118, pp. 327-336.
(12) Abu-Ghannam, B. J. and Shaw, R., Natural Transition of Boundary Layers-The Effects of Turbulence, Pressure Gradients, and Flow History, Journal of Mechanical Engineering Science, 1980, Vol. 22, pp. 231-228.
(13) Schobeiri, M. T., Pappu, K. and Wright, L., Experimental Study of the Unsteady Boundary Layer Behavior on a Turbine Cascade, ASME Paper 95-GT-435, Houston, 1995
(14) Kerrebrock, J. L. and Mikolajczak, A. A., Inter-Stator Transport of Rotor Wakes and Its Effect on Compressor Performance, Trans. ASME Journal of Engineering for Power, 1970, Vol. pp. 359 - 370.
(15) Schlichting, H., Boundary-Layer Theory, 1979, (McGraw-Hill),
(16) Denton, J. D. and Cumpsty, N. A., Loss Mechanisms in Turbomachines, IMechE Paper No. C260/87, 1987
(17) Rotta, J. C., Turbulent Boundary Layers in Incompressible Flow, Pergamon Press, 1962,II, p. 1-219.
(18) White, F. M., Viscous Flow, 1974, (McGraw-Hill).
(19) Costa, J. and Arts, T., Boundary Layer Transition Under the Pressure of Discrete Frequencies in the Freestream Turbulence Spectrum, ASME Paper 91-GT-355, 1991,

APPENDIX

Hereafter summarized are correlations for providing the energy dissipation thickness δ_3 of laminar and turbulent boundary layers. As for the energy dissipation thickness, we have the following equation for the present case (Schlichting[15]) ,

$$\frac{1}{U^3}\frac{d}{dx}\left(U^3\delta_3\right) = \frac{d\delta_3}{dx} = 2C_D \ . \qquad \text{(A.1)}$$

For a laminar boundary layer, dissipation coefficient C_D is given by

$$C_D = \beta Re_\theta^{-1} \ , \quad Re_\theta = \frac{U_\infty \delta_3}{\nu} \ , \tag{A.2}$$

where $\delta_2 = 0.664 x Re_x^{-1/2}$. Adopting $\beta = 0.2$ as suggested by Denton and Cumpsty[16], the integration of Eq. (A.1) finally yields

$$\delta_3 = 1.205 x Re_x^{-1/2} \ . \tag{A.3}$$

For a turbulent boundary layer, Rotta[17] gives

$$\frac{\delta_3}{\delta} \cong \frac{\delta_2}{\delta} + \frac{1}{\kappa^2 \lambda^2}\left(6 + 11.14\Pi + 8.5\Pi^2 + 2.56\Pi^3\right) \ , \quad \Pi = 0.8\left(\beta + 0.5\right)^{0.75} \ , \quad \lambda = \sqrt{\frac{2}{C_f}} \tag{A.4}$$

$$\frac{\delta_2}{\delta} = \frac{1+\Pi}{\kappa\lambda} - \frac{2 + 3.179\Pi + 1.5\Pi^2}{\kappa^2 \lambda^2} \tag{A.5}$$

where β is the Clauser parameter and κ is the Karman constant (=0.41). For simplicity, the other parameters are calculated by the following relationships given by White[18]

$$C_f = 0.025 Re_x^{-1/7}, \quad \delta = 0.14 x Re_x^{-1/7} \ . \tag{A.6}$$

Eq. (A.4) can be approximated with the following expression,

$$\delta_3 = 0.0341 x Re_x^{-1/7} \ , \tag{A.7}$$

where $\beta = 0$.

In the above discussion the boundary layer is assumed to be laminar or turbulent from the leading edge of the flat plate. In order to calculate δ_3 for a boundary layer accompanied with the intermediate transition process, a concept of the virtual origin of the turbulent boundary layer is introduced likewise in the study by Costa and Arts[19]. Assuming that a turbulent boundary layer starts at the virtual origin x_v, then equating Eqs. (A.3) and (A.7) at $x = x_{tr}$, one can obtain the following relation,

$$1.205\left(\frac{\nu x_{tr}}{U_\infty}\right)^{1/2} = 0.0341\left[\frac{\nu\left(x_{tr} - x_v\right)^6}{U_\infty}\right]^{1/7} \ . \tag{A.8}$$

Solving this equation for x_v yields,

$$x_v = x_{tr} - 64.01\left(\frac{\nu^5 x_{tr}^7}{U_\infty^5}\right)^{1/12} \ . \tag{A.9}$$

Consequently, $\delta_{3,L}$ and $\delta_{3,T}$ are given by

$$\delta_{3,L} = \Delta_3\left(x_t\right) \ , \quad \delta_{3,T} = \Delta_3\left(x_{tw}\right) \ , \tag{A.10}$$

where

$$\Delta_3(x) = \max\left[1.205 x_{ref} Re_{x_{ref}}^{-1/2}, 0.0341\left[\frac{\nu\left(x_{ref} - x_v(x)\right)^6}{U_\infty}\right]^{1/7}\right] \ . \tag{A.11}$$